HHS Public Access

Author manuscript

Nature. Author manuscript; available in PMC 2014 November 29.

Published in final edited form as:

Nature. 2014 May 29; 509(7502): 617–621. doi:10.1038/nature13250.

Epidermal Merkel Cells are Mechanosensory Cells that Tune Mammalian Touch Receptors

Srdjan Maksimovic[a,*], **Masashi Nakatani**[a,b,*], **Yoshichika Baba**[a,*], **Aislyn M. Nelson**[a,c], **Kara L. Marshall**[a], **Scott A. Wellnitz**[c], **Pervez Firozi**[c], **Seung-Hyun Woo**[d], **Sanjeev Ranade**[d], **Ardem Patapoutian**[d,e], and **Ellen A. Lumpkin**[a,f,g]

[a]Department of Dermatology, Columbia University, New York, NY 10032

[b]Graduate School of System Design and Management, Keio University, Yokohama, JP

[c]Department of Neuroscience, Baylor College of Medicine, Houston, TX 77006

[d]Howard Hughes Medical Institute, Molecular and Cellular Neuroscience, The Scripps Research Institute, La Jolla CA 92037 USA

[e]Genomic Institute of the Novartis Research Foundation, San Diego, CA 92121 USA

[f]Program in Neurobiology & Behavior, Columbia University, New York, NY 10032

[g]Department of Physiology & Cellular Biophysics, Columbia University, New York, NY 10032 USA

Abstract

Touch submodalities, such as flutter and pressure, are mediated by somatosensory afferents whose terminal specializations extract tactile features and encode them as action potential trains with unique activity patterns[1]. Whether non-neuronal cells tune touch receptors through active or passive mechanisms is debated. Terminal specializations are thought to function as passive mechanical filters analogous to the cochlea's basilar membrane, which deconstructs complex sounds into tones that are transduced by mechanosensory hair cells. The model that cutaneous specializations are merely passive has been recently challenged because epidermal cells express sensory ion channels and neurotransmitters[2,3]; however, direct evidence that epidermal cells excite tactile afferents is lacking. Epidermal Merkel cells display features of sensory receptor cells[4,5] and make "synapse-like" contacts[5,6] with slowly adapting type I (SAI) afferents[7–9]. These complexes,

[¶]Correspondence to: Ellen A. Lumpkin, Ph.D., 1150 St. Nicholas Avenue, room 302B, New York, NY 10032, 212.851.4830, eal2166@columbia.edu.

[*]Equal contribution

Author Contributions

SM screened and analysed transgenic mouse lines, performed and analysed all *ex vivo* optogenic experiments (Fig. 2 and Extended Data Figs. 3–6). MN performed and analysed all whole-cell recordings (Fig. 1, Extended Data Table 1, and Extended Data Fig. 1a & b). YB performed and analysed recordings from *Atoh1* and *Piezo2* strains (Figs. 3 and Extended Data Fig. 8, Extended Data Table 2). AMN performed qPCR (Fig. 1i) and calcium imaging (Extended Data Fig. 1c–i). KLM performed immunhistochemistry in *Atoh1* strains (Extended Data Fig. 7) and assisted in preparation of all figures. SAW and EAL conceived optogenic strategies. PF generated initial ChR2 transgenic mouse lines. EAL conceived and supervised the project. During this manuscript's peer-review process, we entered into a collaboration with SHW, SR and AP, to analyze unpublished $Piezo2^{CKO}$ mice. SR generated $Piezo2^{flox/flox}$ mice, and SHW generated and validated $Krt14^{Cre};Piezo2^{flox/flox}$ mice in AP's lab SM, MN, YB and EAL wrote and AMN, KLM, SAW, PF, SHW and AP edited the manuscript.

which encode spatial features such as edges and texture[1], localize to skin regions with high tactile acuity, including whisker follicles, fingertips and touch domes. Here, we show that Merkel cells actively participate in touch reception in mice. First, Merkel cells display fast, touch-evoked mechanotransduction currents. Second, optogenetic approaches in intact skin show that Merkel cells are both necessary and sufficient for sustained action-potential firing in tactile afferents. Third, recordings from touch-dome afferents lacking Merkel cells demonstrate that Merkel cells confer high-frequency responses to dynamic stimuli and enable sustained firing. These data are the first to directly demonstrate a functional, excitatory connection between epidermal cells and sensory neurons. Together, these findings indicate that Merkel cells actively tune mechanosensory responses to facilitate high spatio-temporal acuity. Moreover, our results suggest a division of labour in the Merkel cell-neurite complex: Merkel cells signal static stimuli, such as pressure, whereas sensory afferents transduce dynamic stimuli, such as moving gratings. Thus, the Merkel-cell neurite complex is unique sensory structure with two receptor cell types specialized for distinct elements of discriminative touch.

We first asked whether Merkel cells display touch-activated currents. Merkel cells from *Atoh1/nGFP* mice were purified by flow cytometry for whole-cell recordings[10] (Fig. 1a–b). Merkel cells showed displacement-dependent inward currents (Fig. 1c–d) whereas keratinocytes lacked mechanosensitive currents over the same stimulus range (N=4). Merkel-cell currents averaged 370±80 pA at peak and 20±6 pA at steady state (Extended Data Fig. 1 and Table 1). They displayed steep displacement-operating ranges (1.6±0.1 μm; Fig. 1d and 1e) and millisecond rise times (Fig. 1f and Extended Data Table 1), which were limited by stimulus-probe velocity. This suggests fast gating mechanisms, similar to force-gated channels in hair cells and invertebrate mechanosensory neurons[11].

We next asked whether biophysical properties of touch-activated currents matched those of identified mechanosensitive channels. Currents showed fast inactivation time constants (8±2 ms; Fig. 1g), similar to those of dorsal root ganglia (DRG) neurons[12]. Mechanotransduction currents showed a linear current-voltage relation (reversal potential, 8±3 mV, Fig. 1h), indicating non-rectifying, non-selective cation channels. Moreover, they were attenuated by Ruthenium Red (RR; Extended Data Fig. 1). These biophysical properties are consistent with mechanosensitive channels encoded by *Piezo* genes (Piezo2: $\tau_{inactivation}$=7±1 ms; E_{rev}=9±2 mV; RR block ~80%)[13]. Indeed, quantitative PCR analysis showed that Merkel cells express *Piezo1* and *Piezo2*, and that *Piezo2* is enriched in Merkel cells compared with epidermis (Fig. 1i).

Merkel cells also exhibited robust touch-evoked increases in cytoplasmic Ca^{2+} (Extended Data Fig. 1). As these cells were not voltage clamped, calcium signals likely reflected calcium entry through mechanotransduction channels, opening of voltage-activated calcium channels and subsequent calcium-induced calcium release, as is the case for hypotonic-activated responses in Merkel cells[10]. Collectively, our findings demonstrate for the first time that Merkel cells are capable of transducing touch stimuli into excitatory responses in the absence of sensory neurons or keratinocytes.

How might the Merkel cell's rapidly inactivating mechanotransduction currents lead to slowly adapting responses *in vivo*? Like hair cells and *Drosophila* bristles[14] Merkel-cell

mechanotransduction channels display steady-state currents that are ~10% of peak responses (Extended Data Fig. 1). These currents are likely to be amplified by voltage-activated calcium channels[4,10]. Indeed, an accompanying manuscript demonstrates that inward currents of ≤20 pA are sufficient to depolarize Merkel cells to voltage-activated ion-channel thresholds[15]. Moreover, computational modelling predicts that a rapidly adapting transduction current with a small steady-state component can account for SAI firing patterns[16]. Finally, each SAI afferent innervates a cluster of Merkel cells, whose contributions will be integrated at spike initiation zones.

We next tested whether activating Merkel cells in the intact skin is sufficient to excite tactile afferents. We used optogenetics to selectively depolarize Merkel cells without directly stimulating their associated sensory afferents (Fig. 2a). A previous microarray screen identified cholecystokinin (CCK) as a Merkel cell-specific transcript in the epidermis[4]. To express Channelrhodopsin-2[17] (ChR2) in Merkel cells *in vivo*, we crossed Cck-IRES-Cre mice[18] with mice harboring a ChR2-tdTomato fusion at the *Gt(Rosa)26Sor* locus[19]. Heterozygote $Cck^{Cre/+};ChR2^{loxP/+}$ mice showed strong expression of ChR2-tdTomato in touch-dome Merkel cells, whose fluorescence was easily identifiable in intact skin (Fig. 2b). Whole-cell recordings *in vitro* confirmed that $ChR2^{+}$ Merkel cells exhibited light-activated inward currents (*N*=5, Extended Data Fig. 2). We confirmed the absence of ChR2 expression in SAI afferents via immunohistochemistry of skin cryosections (Fig. 2c) and whole-mounts (Extended Data Fig. 3a–e). ChR2 expression was not observed in any cutaneous afferent (*N*=21 mice). Epidermal ChR2-tdTomato expression was limited to Merkel cells; however, ChR2-tdTomato was observed in some dermal cell types (Extended Data Figs. 3).

To acquire touch-dome specific responses, we used laser-coupled fibre optics with a collimator lens to restrict illumination to touch domes (Fig. 2d). When touch domes were presented with 5-s light pulses, action potentials were observed in phase with light stimulation (Fig. 2e). All afferents that displayed light-evoked responses were touch-sensitive (*N*=12), and were classified as SAI afferents based on physiological criteria. We confirmed that the touch- and light-evoked activity derived from single units with multidimensional spike-sorting[20] and by comparing spike waveforms (Fig. 2e′). Light-evoked responses showed increased firing with increased light intensities (Fig. 2f–f′). Illumination of tissue that lacked Merkel cells, including skin areas adjacent to touch domes and saphenous nerve trunks, did not evoke action potentials (Extended Data Fig. 4). Illumination of touch domes with green light (545 nm), which does not activate ChR2, also failed to elicit afferent firing. Light-evoked responses from SAI afferents (*N*=3 units) were also observed when ChR2-tdTomato expression was driven by the epidermis-specific $K14^{Cre}$ locus[21] (Extended Data Fig. 5), confirming that light-evoked responses requires the presence of ChR2-expressing epidermal cells. Thus, we conclude that depolarization of epidermal Merkel cells is sufficient to excite action potentials in SAI afferents. To our knowledge, this is the first functional proof of an excitatory connection between any epidermal cell type and tactile afferents in skin.

In SAI afferents, touch stimuli elicit biphasic responses with a dynamic phase characterized by high-frequency firing at touch onset, and a static phase characterized by sustained firing

with highly variable inter-spike intervals (ISIs)[7–9]. To test whether Merkel-cell photostimulation recapitulated these properties, we recorded action potential trains elicited by 3-min light stimuli (Fig. 2g–h). In excellent agreement with canonical SAI responses[7–9], light-evoked responses showed continuous firing throughout stimulation with coefficients of variation (CoV) of ISIs >0.5 (mean±SD, 1.17±0.14, *N*=12). Interestingly, light-evoked responses lacked high-frequency firing at stimulus onset (*e.g.*, Fig. 3a–b). Thus, selective activation of epidermal Merkel cells is sufficient to elicit action potential trains whose activity patterns mimic the static phase of touch-evoked SAI responses.

We next tested whether optogenetic silencing of Merkel cells inhibits touch-evoked firing in SAI afferents. We selectively expressed Archaerhodopsin-3 (ArchT), a green-light-sensitive, hyperpolarizing proton pump[22], in Merkel cells (*Cck*$^{Cre/+}$;*ArchT*$^{loxP/+}$; Extended Data Fig. 6). During 3-min displacements, touch domes were presented with a series of 10-s light pulses. We observed a tenfold reduction in median touch-evoked firing rates during light stimuli (*N*=3; Fig. 2i–j). Inhibition grew progressively stronger during sustained displacement, becoming almost complete with successive light presentations (Fig. 2i). Thus, Merkel-cell depolarization is necessary for robust static phase firing in SAI afferents.

To determine whether Merkel cells also contribute to the dynamic phase of touch-evoked SAI responses, we analysed epidermal-specific *Atoh1* conditional knockout (*Atoh1*^{CKO}) mice (*K14*^{Cre};*Atoh1*$^{LacZ/flox}$), which completely lack Merkel cells[23]. Touch domes were innervated by myelinated afferents that contain nodes of Ranvier, suggesting that they are capable of firing action potentials (Extended Data Fig. 7). A previous unbiased survey of touch-sensitive afferents reported a selective loss of SAI responses in *Hoxb1*^{Cre};*Atoh1*$^{Flox/LacZ}$ mice, which lack Merkel cells from development but retain innervation of touch domes and footpads[24]. Here, we used a targeted approach to analyse firing properties of afferents that selectively innervate touch domes, which were identified during recording based on FM1-43 uptake[25]. We found that touch domes in *Atoh1*^{CKO} mice were innervated by mechanosensitive Aβ afferents (conduction velocity: 10.2–18.5 m/s; *N*=6); however, their firing patterns differed markedly from SAI responses[8,9] in control genotypes (Fig. 3a–b; *N*=5). First, static phase firing was truncated in *Atoh1*^{CKO} mice compared with control afferents, which maintained firing throughout 5-s stimuli (Fig. 3a–b). Thus, responses of *Atoh1*^{CKO} touch-dome afferents could be classified as intermediately adapting[9,26] (IA; Fig. 3c). Second, *Atoh1*^{CKO} responses displayed spike counts (Fig. 3d and Extended Data Table 2 and firing rates that were markedly lower than control genotypes (mean±SD: *Atoh1*^{CKO}: 25±8 Hz, Control: 59±25 Hz; P=0.004). Notably, *Atoh1*^{CKO} lacked high-frequency firing and short ISIs in both dynamic and static phases (peak firing rates: *Atoh1*^{CKO}: 79±40 Hz; Control: 238±69 Hz; P=0.003; Extended Data Fig. 8 and Extended Data Table 2). Together, these data indicate that touch-dome afferents have mechanosensory terminals capable of responding to touch, but do so with substantially altered firing properties.

We next compared the responses of touch-dome afferents in *Atoh1*^{CKO} with epidermal-specific *Piezo2* knockout mice[15] (*Piezo2*^{CKO}). In the latter, Merkel cells and touch-dome afferents develop normally and are retained through adulthood[15]. Although these mutations disrupt distinct molecular pathways and cause different anatomical phenotypes, we found a

remarkable degree of concordance between static-phase firing patterns. Mutant touch-dome afferents displayed a similar proportion of IA responses (Fig. 3c)[15] and showed similar increases in mean ISIs during static displacement (Fig. 3e and Extended Data Fig. 8). Together, these data indicate that Piezo2-dependent Merkel-cell signaling is essential for proper SAI responses to sustained pressure.

Our study sheds new light on the role of Merkel cells in touch reception. Our findings demonstrate that Merkel cells are touch-sensitive cells that actively tune mechanosensory afferents by conferring two features of the SAI response: sustained responses and high-freqency firing. First, by maintaining firing throughout mechanical stimulation, SA afferents inform the brain about pressure[1,27]. Our optogenetic approach demonstrates that Merkel-cell activation elicits, and silencing reversibly suppresses, sustained SAI firing. This provides the first direct evidence that Merkel cells are not simply passive mechanical filters in the skin. Moreover, recordings from *Atoh1*^{CKO} and *Piezo2*^{CKO} mice show that SAI afferents cannot properly convey static phase information without intact Merkel cells. Second, during active tactile exploration, high-frequency firing is important for encoding object features (*e.g.,* edges and curvature) with high information content[27,28]. Although touch-dome afferents in *Piezo2*^{CKO} showed similar dynamic responses to control mice, *Atoh1*^{CKO} afferents showed markedly reduced dynamic firing. Thus, Merkel cells perform *Piezo2*-independent functions that enhance dynamic responses, which is predicted to facilitate high spatio-temporal acuity of tactile perception. Consistent with this prediction, *Atoh1*^{CKO} mice display behavioral deficits in texture preference[29]. These effects might be due to differences in SAI afferent development, touch-dome mechanics or *Piezo2*-independent signalling mechanisms.

How might Merkel cells contribute to the SAI afferent's unique firing patterns? Our findings suggest two new models for touch reception. First, the Merkel cell-neurite complex is a compound sensory system with two receptor cell types that mediate different aspects of touch transduction[30] (Fig. 4). A similar division is found in the visual system, which also provides information on object shape and movement. In retina, rods are optimized for low-light conditions and cones for high-acuity, color vision. Second, the contribution of Merkel cells to dynamic firing indicates that they could function in signal amplification, analogous to outer hair cells in the mammalian cochlea. These mechanosensory cells actively expend energy to tune the cochlea's frequency selectivity and mechanical sensitivity. A key question that remains is the nature of the excitatory mechanisms that convey signals between Merkel cells and SAI afferents.

Methods

Experimental Animals

All experimental procedures followed National Institute of Health guidelines and were approved by Columbia University Institutional Animal Care and Use Committee (IACUC). Preliminary studies performed at Baylor College of Medicine (BCM) were approved by the BCM IACUC.

Optogenetic experiments were performed on 6–10 week old male and female mice. For optogenetic activation of Merkel cells, *Cck*$^{Cre/+}$;*ChR2*$^{loxP/+}$ and *K14*^{Cre};*ChR2*$^{loxP/+}$ mice

were generated by crossing Ai27D mice (B6.Cg-*Gt(ROSA)26Sor*$^{tm27.1(CAG-COP4*H134R/tdTomato)Hze/J}$), which conditionally express a ChR2-tdTomato fusion protein from the *Gt(Rosa)26Sor* locus[19], with one of two Cre-expressing strains. For *Cck*$^{Cre/+}$;*ChR2*$^{loxP/+}$, we used Cck-IRES-Cre mice (*Cck*$^{Tm1.1(Cre)Zjh/J}$), a knock-in mouse line that expresses Cre recombinase directed by the endogenous Cholecystokinin (*Cck*) promoter/enhancer elements[18]. For *K14*^{Cre};*ChR2*$^{loxP/+}$, transgenic K14-Cre (*Tg*$^{KRT14\text{-}cre}$*1Amc/J*) mice[21] were used. For optogenetic inhibition of Merkel cells, *Cck*$^{Cre/+}$;*ArchT*$^{loxP/+}$ mice were generated by crossing Cck-IRES-Cre mice[18] with B6.Cg-*Gt(ROSA)26Sor*$^{tm40.1(CAG-AOP3/EGFP)Hze/J}$ mice, which conditionally express a ArchT-EGFP fusion protein from the *GT(Rosa)26Sor* locus (MGI Ref. ID: J:191265).

Atoh1 conditional knockout (*Atoh1*^{CKO}) mice were generated as described previously[23]. Mice of the *K14*^{Cre};*Atoh1*$^{\text{LacZ/flox}}$ genotype lacked expression of *Atoh1* in *K14*-expressing cells and were designated as *Atoh1*^{CKO} mice. Genotypes that lacked either Cre and/or LacZ were designated as controls. Female mice (8–15 week old) were used for experiments.

Piezo2^{CKO} and control genotypes were generated as described in the accompanying manuscript[15]. Female mice (6–19 weeks) were used for experiments.

For whole cell patch clamp experiments, Merkel cells were dissociated from male and female *Atoh1/nGFP* pups (P2-P5)[31] and *Cck*$^{Cre/+}$;*ChR2*$^{loxP/+}$ pups (P5).

Immunohistochemistry

For cryosections, mouse skin was shaved, depilated (Surgi-cream) and dissected either from the back or from the hind limb of *Cck*$^{Cre/+}$;*ChR2*$^{loxP/+}$ mice or from female *Atoh1*^{CKO} mice and littermate controls (8–10 weeks of age). Tissue was fixed in 4% paraformaldehyde (PFA), cryoprotected in 30% sucrose, frozen and sectioned at a thickness of 16–20 μm. Cryosectioned skin was labelled at 4°C overnight with primary antibodies against Keratin-8 (TROMA1, DSHB, 1:100), Neurofilament H (Abcam: ab4680, 1:2000), Nestin (Aves Labs, NES, 1:200), S100 (Dako, Z0311, 1:500) or βIV spectrin (Gift from Dr. Matthew Rasband, 1:200[32]). Secondary goat AlexaFluor-conjugated antibodies (Invitrogen) directed against rat (Alexafluor 488; A11006), chicken (Alexafluor 647; A21449), rabbit (Alexafluor 488; A11034) IgG were used for 1 h at room temperature (1:1000).

For whole-mount immunostaining, skin pieces (2–5 mm in diameter) containing two to five touch domes (recorded and neighbouring touch domes) were dissected from the skin-saphenous nerve preparation after *ex-vivo* recording. The following steps were all performed at 4°C: Tissue was fixed in 4% paraformaldehyde (PFA) for 2–4 hours and blocked overnight with 5% normal goat serum containing 0.3% TritonX-100 (5% NGST) + 10% DMSO + M.O.M. blocking reagent (Vector Labs, MKB-2213, 2 drops/ml). The next day tissue was washed with PBS containing 0.3% TritonX-100 (PBST) for several hours and incubated with primary antibodies in 5% NGST for 3–6 days. Primary antibody concentrations were the same as indicated for cryosections. After four washes (30 min to 1 h each) with PBST, tissue was incubated with secondary antibodies in 5% NGST for two days (1:500). After four washes with PBST (30 min to 1 h each), skin was dehydrated in serial tetrahydrofuran solutions and cleared in dibenzyl ether, according to published methods[33].

Skin was imaged in dibenzyl ether by confocal microscopy (Zeiss exciter equipped with 20X, 0.8NA and 40X 1.3 NA objective lenses). For whole mounts, we used the same antibodies as for cryosections, plus an additional two: primary antibody against Neurofilament 200 (Sigma-Aldrich, N0142, 1:300); secondary antibody against mouse IgG (Invitrogen, Pacific Blue, P31582).

In vitro electrophysiology

The Merkel cell isolation and patch clamp recording procedure were described previously[10]. Currents were recorded from Merkel cells after 1–2 days in culture with an Axopatch 200B amplifier, a Digidata 1440A interface and a personal computer running pClamp 10 software (Axon Instruments). Pipette resistance ranged from 0.9–3.5 MΩ. The perforated patch technique was used for all whole-cell recordings. Pipette tips were filled with internal solution and backfilled with internal solution supplemented with 100–180 μg/ml Amphotericin B (Sigma-Aldrich). After a gigaohm seal was established, the series resistance decreased to 10–20 MΩ within 5 min. Membrane capacitance was measured from the decay constant during a 1 ms voltage step using pClamp software. Signals were filtered at 5 kHz and digitized at 25 μs. Leak currents were compensated during whole-cell recordings with a P/6 leak subtraction protocol. Currents in the whole-cell configuration were recorded in extracellular solution containing (in mM): 140 NaCl, 5 KCl, 10 HEPES (pH 7.4, adjusted with NaOH), 10 D-glucose, 2 $MgCl_2$, and 2 $CaCl_2$. The pipette solution contained (in mM): 70 KOH, 70 KCl, 10 NaCl, 1 $MgCl_2$, 0.5 $CaCl_2$, 5 EGTA, 2 MgATP, and 10 HEPES (pH 7.2, adjusted with D-gluconate).

The somata of dissociated Merkel cells were stimulated for 50 ms by families of displacements (0.3-μm steps) every 5 s, with a glass probe (tip diameter: 2–3 μm) driven by a piezoelectric actuator (model PA8/12; Piezosystem Jena; power supply ENV40 C; Piezosystem Jena). The glass probe was positioned at an angle of 48° to the cover slip. Displacements were triggered by a pClamp-controlled command voltage passed to the actuator driver through a low-pass filter (f_{cutoff}: 500 Hz; model LPF-100A, Warner Instruments). The rise time of the driving signal was 0.6±0.1 ms, calculated as the latency for the probe to travel 10–90% of a half-maximal displacement. The speed of the mechanical stimulator was 2 μm/ms. In combination with the rise time of the driving signal, the latency of the stimulator was estimated at ~1 ms. Mechanically evoked currents were measured at a holding potential of −70 mV. We chose dendritic Merkel cells for recordings, which typically show fast activation and inactivation kinetics (Fig. 1c). In addition, mechanosensitive currents with fast activation kinetics were occasionally recorded from oval-shaped Merkel cells. These tended to show both fast (<10 ms) and slow inactivation kinetics (10–200 ms).

Displacement magnitudes were visually calibrated daily. To ensure that mechanosensitive channels were not activated at rest, displacements began from an offset position located 1–2 μm away from the soma[34]. Thus, each stimulus family included ~6 displacements that did not contact the soma. To correct for this variable offset, displacements are reported relative to each cell's mechanical threshold (labelled as "0" in Fig. 1d). Mechanical threshold was defined as the displacement that elicited a peak current ≥4 times the SD of the pre-stimulus

noise level (12.5 ms before stimulus onset). For clarity, this offset has been subtracted from the stimulus families shown in Fig. 1d.

Given that stimulus-response relations are normalized to each cell's mechanical threshold, their lateral shifts likely reflect a compliance in series with mechanotransduction machinery. One possibililty is the coupling between the cell and the coverslip, which was not systematically controlled in these *in vitro* recordings.

Current-displacement relationships were fitted for the normalized current with a Boltzmann equation of the form: $I_{norm}(x)=1/(1+\exp(-((x-x_{50})/s))$, where x is the displacement (in μm), x_{50} is the displacement that produces half-maximal amplitude of the peak current, and s is the current sensitivity to displacement. For estimating the activation kinetics, the period from 10 to 90% of a maximal evoked current was calculated and denoted as rise time $t_{10–90\%}$. For estimating the inactivation kinetics, single-exponential fitting was conducted with Clampfit for 47 and 50 ms from peak current time point for touch- and light-evoked current, respectively. Both activation and inactivation kinetics where the displacement was x_{50} were estimated by linear interpolation of adjacent four points. For calculating the operating range, we adopted the method used to study hair cells: the operating range of the $I_{norm}(x)$ relation was the net deflection required to evoke from 10 to 90% of the maximum response[35]. To estimate reversal potential, mechanical stimuli were delivered at multiple holding potentials (−75 to +50 mV in 25 mV increments). Holding potentials were stepped 150 ms prior to mechanical stimulation (50 ms).

For the Ruthenium Red blockade experiment, 50 mM stock solution was prepared in DMSO and dissolved into extracellular solution at a final concentration of 100 μM. Mechanical stimulation was given at least five times after reaching the mechanical threshold of each Merkel cell. To quantify the blocking effects of Ruthenium Red, we compared maximal inward current (peak current (I_{peak}), averaged from a 250-μs time window), with current at the end of touch stimulation (steady state current (I_{ss}), averaged from a 5-ms time window).

FM1-43 Dye Injections

FM1-43 (Biotium; #70020) was used to visualize SAI receptive fields (touch domes) in *Atoh1-nGFP* and *Atoh1*^{CKO} mice. FM1-43 was diluted at 1.5 mM in sterile PBS and injected subcutaneously (70 μl per mouse). Hindlimb skin for *ex vivo* skin-nerve electrophysiology was harvested 12–14 h after injection.

Ex vivo skin-nerve electrophysiology

Light- and touch-evoked responses in the skin were recorded after dissecting the hindlimb skin and saphenous nerve according to published methods[9]. Briefly, the skin was placed epidermis-side-up in a custom chamber and perfused with carbogen-buffered synthetic interstitial fluid (SIF) kept at 32°C with a temperature controller (model TC-344B, Warner Instruments). The nerve was kept in mineral oil in a recording chamber, teased apart and placed onto a silver recording electrode connected with a reference electrode to differential amplifier (model 1800, A-M Systems). The extracellular signal was digitized using a DT304 A/D board (DataWave Technologies) and recorded using Sci-Works Experimenter software

(DataWave Technologies). SAI receptive fields (touch domes) were visualized using a fluorescence microscope equipped with tdTomato (for *Cck*$^{Cre/+}$;*ChR2*$^{lox/P}$ and *K14*^{Cre};*ChR2*$^{lox/P}$ mice) and GFP (for *Cck*$^{Cre/+}$;*ArchT*$^{loxP/+}$, *Atoh1/nGFP* and *Atoh1*^{CKO} mice) filter sets. Light stimuli were delivered with a fiber-optic coupled blue laser, and a stereomicroscope coupled with a Xenon arc lamp (described below).

For these studies, we focused on touch-dome afferents, which innervate Merkel cells in wildtype animals, as described by Iggo and Muir[7]. The afferents generally have no spontaneous firing, respond selectively to pressure applied directly to a touch dome, are particularly sensitive to moving stimuli but are insensitive to hair tugging and skin stretch[7]. To identify responses from these afferents in mutant and control genotypes, we used a mechanical search paradigm with a fine glass probe. Afferents were classified as 'touch-dome afferents' according to the following criteria: 1) Aβ conduction velocity (≥9 m/s), 2) punctate receptive fields restricted to one or more fluorescently labeled touch domes, 3) insensitive to pressure applied to skin areas adjacent to touch domes, 4) insensitive to hair tugging but responsive when the hair is bent to compress the touch dome. Touch-sensitive afferents that did not meet these criteria were not analyzed further. Responses were classified as intermediately adapting (IA) if firing ceased during the first 4 s of the static phase, and slowly adapting (SA) if spikes were observed throughout the duration of the 5-s hold phase.

Recordings and analysis of *Piezo2*^{CKO} and their controls were performed blind to genotype. For other strains, directed recordings could not be performed blind to genotype because transgenic and control Merkel cells differed in the appearance under the fluorescence microscope used to confirm the presence of touch domes in the receptive field. In the *Atoh1*^{CKO} strain, FM1-43 labelling differs from control mice because the former lack FM1-43-labeled Merkel cells[24] (Extended Data Fig. 7). In transgenic mice expressing ChR2 or ArchT, the presence of fluorescent Merkel cells was confirmed for each touch dome analysed.

Mechanical responses were elicited with von Frey monofilaments and a custom-built mechanical stimulator. The automated mechanical stimulator applied stimuli with an indenter (tip diameter: 1.6 mm), and stimuli were commanded using a model XPS comitial motion controller and driver system (Newport) connected to a PC computer. Movement of the indenter was controlled with custom-made software and measured with a laser distance-measuring device (OptipNCDT 1402, Micro-Epsilon). Touch stimuli consisted of ramp and 5-s hold indentations. First-order approximation of approach speed was 3.2 mm/s. Mechanical displacements ranged from 0.4–1.6 mm in depth. The period between successive displacements was 60–70 s. For optogenetic silencing, mechanical stimulation was delivered with a glass probe (tip diameter ~50 μm) mounted on a mechanical stimulator.

Conduction velocity was measured by electrically stimulating identified receptive fields. Spike sorting and data analysis were done off-line in MATLAB and Wave clus[20].

Optical stimulation

For *ex vivo* electrophysiology of $Cck^{Cre/+}$;$ChR2^{loxP/+}$ and $K14^{Cre}$;$ChR2^{loxP/+}$ mice, light responses were evoked with a fibre-optic-coupled DPSS laser (473 nm; model BL473T3-150FC, Shanghai Laser & Optics Century Co.). A collimator lens was mounted on the end of the optical fibre (100 μm core) to prevent lateral spread of the light stimulus. The light source was positioned one focal distance above the skin so that the light stimulus (150–200 μm in diameter) was focused when projected on the touch dome. Light intensity was measured with a PM100USB power meter (Thorlabs). Duration of light stimuli was controlled via TTL delivered from a pulse stimulator (model 2100, A-M Systems). To reconstruct intensity-response curves we used 5-s light flashes of seven different intensities. All recordings were performed in low-light conditions and a period between successive illuminations (30 s) allowed for ChR2 recovery after desensitization[36]. To test sustained light responses, we used 3-min constant illuminations of 50 μW.

For *ex vivo* electrophysiology of $Cck^{Cre/+}$;$ArchT^{loxP/+}$ mice, inhibitory green-light pulses were delivered by the LAMBDA LS Xenon Arc Lamp (Sutter Instruments) coupled to a stereoscopic microscope (Olympus) equipped with a 545-nm (30-nm half-width) excitation filter. Recorded touch domes were positioned in the center of the illuminated field (5-mm diameter). Displacements (3 min) were delivered with a small glass probe (tip diameter ~50 μm). To inhibit Merkel-cell activity we used a constant intensity of 50 mW/cm^2 (measured at 545-nm). Duration of 10-s light pulses was monitored with a photodiode. The period between successive illuminations was also 10 s. Each recording started with a 10-s light-off period and then light-on and -off periods alternated. Every recording ended with a light-on period. The dynamic phase (first 10 s) was not included in the calculation in Fig. 2j.

To acquire light-evoked current from isolated Merkel cells that expressed ChR2, blue light stimulation was given by the LAMBDA XL light source (Sutter Instruments) for 50 ms, controlled by Metafluor software (version 7.6.3, Molecular Devices). The holding potential was −70 mV. The expression of ChR2-tdTomato in Merkel cells was visually confirmed before approaching with the pipette. 100 nM all trans-Retinal was added into extracellular solution just before recording.

Live-cell calcium imaging

After two days in culture, Merkel cells were loaded for 30 min with 3 μM fura-2 acetoxymethyl ester (Molecular Probes) in a modified Ringer's solution (in mM): 140 NaCl, 5 KCl, 10 HEPES (pH 7.4), 10 D-Glucose, 2 $MgCl_2$, and 2 $CaCl_2$ (osmolality: 290 mmol·kg −1). Cells were given 30 min in extracellular solution to digest the ester bonds before imaging. Merkel cells were depolarized with high potassium extracellular solution containing (in mM): 75 NaCl, 70 KCl, 10 HEPES (pH 7.4), 10 D-glucose, 2 $MgCl_2$, and 2 $CaCl_2$ (osmolality: 290 mmol·kg^{-1}) as a positive control. Data were acquired with Metafluor software (version 7.6.3, Molecular Devices), and analysed with custom programs written in Igor Pro (version 5.03, Wavemetrics). Displacements (2–3 μm) were applied with a stepper motor.

Quantitative PCR analysis

Complementary DNA was synthesized with oligo-dT primers and SuperScript III (Invitrogen) from pooled Merkel cells according to published protocols (~25,000 Merkel cells collected from six P3-4 pups[37]). Keratinocytes were harvested from three P3-4 pups and were assayed as total epidermal cell suspensions. Primers were designed with Primer3 (http://biotools.umassmed.edu/bioapps/primer3_www.cgi). Primer pairs were optimized for qPCR and validated for specificity and sensitivity in control specimens. Standardized SYBR Green amplification protocols were used on the StepOnePlus Real-time PCR System (Applied Biosystems) as suggested by the manufacturer. All gene expression experiments.used 30 ng of cDNA. Melting curves were generated for all products to confirm a single amplicon for each product. To determine gene expression in each sample, cycle thresholds (C_T) of the gene of interest were normalized to the reference gene GAPDH (ΔC_T). Quantitative PCR experiments were peformed twice, with four technical replicates per experiement. Primer sequences were:

GAPDH	5′ CACAATTTCCATCCCAGACC 3′ 5′ GTGGGTGCAGCGAACTTTAT 3′
KRT14	5′ AGATGGAGCAGCAGAACCAG 3′ 5′ CAGGAAGGACAAGGGTCAAG 3′
KRT1	5′ ATTGCTGCGTGACTTCCAG 3′ 5′ GGCTACTGCTTCCGCTCA 3′
Atoh1	5′ CCCACAGAAGTGACGGAGAG 3′; 5′ GAGGAAGGGGATTGGAAGAG 3′
Piezo1	5′ GGAAGAGGACTACCTTGGTG 3′ 5′ GCTGACCTTGTCACTGAAGA 3′
Piezo2	5′ CTTGTGAGGTCGGGTGGT 3′ 5′ ATGAGGGGATGGGGAGAG 3′

Statistics and sample sizes

Fisher's exact test was used to evaluate differences in afferent populations (Fig. 3c). Differences between population means were assesed with unpaired Student's *t* test (two tail) for normally distributed data. Since fewer than 10 afferents were included in Figs. 3d–e and Extended Data Fig. 8, we also used two-tail Mann-Whitney test, which confirmed that medians of populations indicated with asterisks were statistically different ($P<0.001$ for all comparisons). Variances between control and mutant genotypes were not statistically different, with the exception of static-phase ISIs from *Piezo2*^{CKO} mice ($P<0.01$; U value=1, Mann-Whitney).

Sample sizes were chosen based on published and pilot studies. For *in vitro* electrophysiology, we conducted pilot studies to measure touch-activated currents in four Merkel cells. Power analysis showed that at least two recordings are sufficient to discriminate touch activated currents from voltage- and calcium-activated potassium currents, which are the majority of transmembrane currents measured in a previous study[10]. For optogenic Merkel-cell silencing, the sample size was limited by the number of adult animals available for *ex vivo* skin-nerve preparation recording. For *ex vivo* recordings from *Atoh1*^{CKO} and *Piezo2*^{CKO} mice, we based samples sizes on our previous survey of touch-

sensitive afferents in Atoh1^{CKO} mice[24]. Among Aβ afferents, we observed eight SAI afferents in control mice (n=8/39) but none in *Atoh1*^{CKO} genotypes (n=0/27)[24]. Thus, we reasoned that at least five afferents per group would be sufficient to observe differences in response properties of touch-dome afferents in directed recordings.

Extended Data

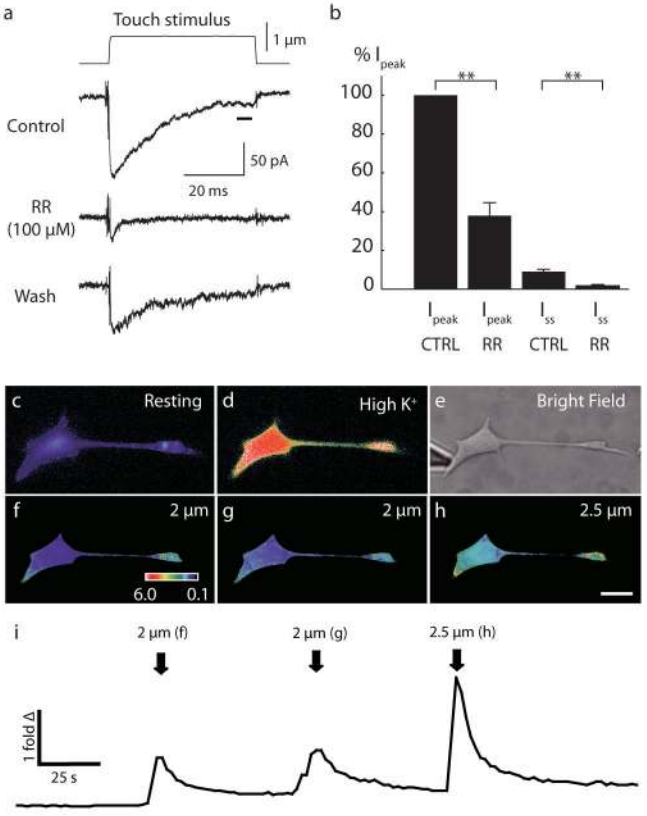

Extended Data Figure 1. a–b, Mechanically activated currents in Merkel cells were inhibited by Ruthenium Red (RR)

a, Representative trace of mechanically evoked current induced by 1-µm mechanical displacement. Application of RR (100 µM) attenuated mechanically activated current. **b,** Peak currents (I_{peak}) were estimated from 250 µs around peak and steady-state currents (I_{ss}) were estimated from the last 5 ms (black bar in **1a**) of mechanical displacements. Data were normalized by I_{peak} for each cell. With Ruthenium Red, I_{peak} was reduced to 38±7% of control condition. Steady state currents were also reduced by RR (*N*=4; control: 9±1% of I_{peak}; RR: 2±1% of I_{peak}). **c–i,** Merkel cells display reversible Ca^{2+} responses to focal displacements applied to somata. **c,** Representative pseudocolor images of fura-2 ratios (340:380) of a Merkel cell at rest. **d,** A Merkel cell activated by depolarizing (high-K^+) solution. **e,** A brightfield image showing the position of the stimulus probe. **f–h,** Peak responses corresponding to each displacement. 'Fold Δ' is the fold change in fluorescence ratio from baseline. Scale bar, 10 µm. **i,** Representative time course of mean fura-2 ratios during the touch stimuli shown above. Stimulus onset in **f–h** is indicated by arrows. Calcium responses were stimulus dependent. Similar responses were observed from 11 Merkel cells.

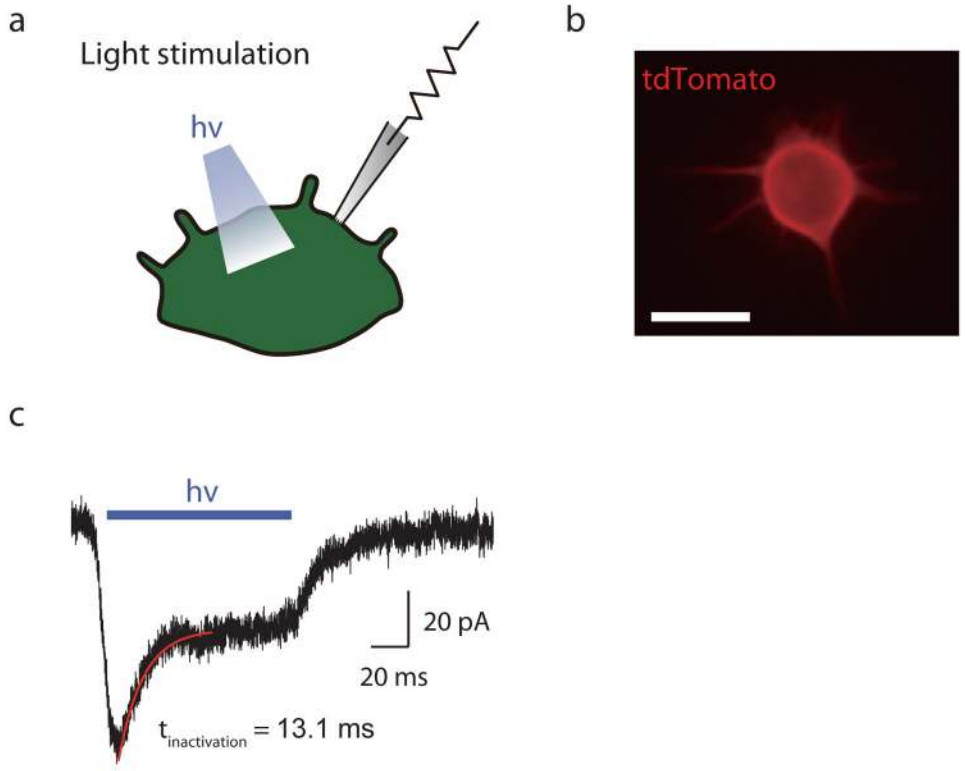

Extended Data Figure 2. ChR2^{+} Merkel cells display light-activated inward currents

a, Light-activated currents were recorded with whole-cell, tight-seal voltage clamp methods. **b,** Fluorescent image of a ChR2-tdTomato expressing Merkel cell. Scale bar, 10 μm. **c,** Representative trace for light-activated inward currents at a holding potential of −70 mV. Inactivation kinetics were measured by fitting a single exponential curve (red).

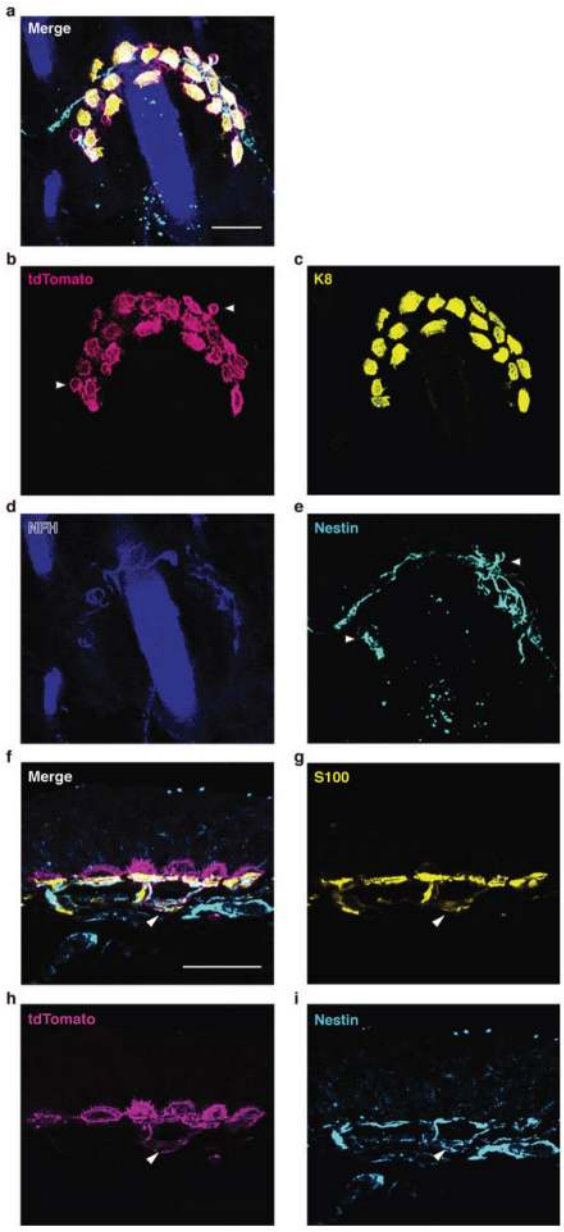

Extended Data Figure 3. Immunostaining of ChR2-expressing touch domes

a–e, Whole-mount staining and confocal axial projection of the touch dome shown in Fig. 2d. a, Merged image. **b–d,** Expression of ChR2-tdTomato was present in Merkel cells (Keratin-8, K8), but absent from sensory terminals (Neurofilament Heavy, NFH). **e,** Some terminal Schwann cells (Nestin)[38] also expressed ChR2 (arrowheads in **b** & **e**). **f–i,** Immunostaining of skin cryosections. **f,** Merged image. **g–i**, ChR2-tdTomato was present in some $S100^{+}$ Schwann cells that also expressed Nestin, a marker for type II terminal Schwann cells[38] (arrowheads in **f–i**). Scale bars, 20 μm.

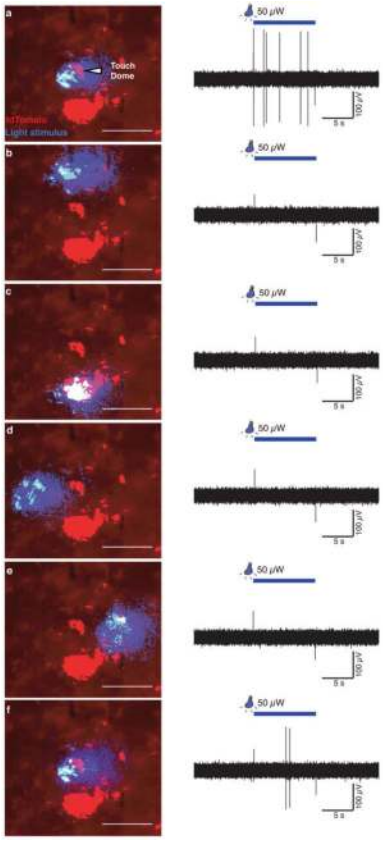

Extended Data Figure 4. Light-evoked activity is specific to touch-dome illumination

a & f, Responses to light stimuli centred on a touch dome. **b–e**, When the light stimulus was positioned around the touch dome, no light-evoked activity is observed. Illuminating a cluster of ChR2^{+} dermal cells did not evoke any responses (**c**). **f**, To confirm that the absence of light-evoked activity was not due to the loss of Merkel cells and/or neuronal fibres, the experiment ended by re-positioning the light stimulus over the touch dome to re-elicit light-evoked activity. Images have been thresholded for clarity. Scale bars, 200 μm.

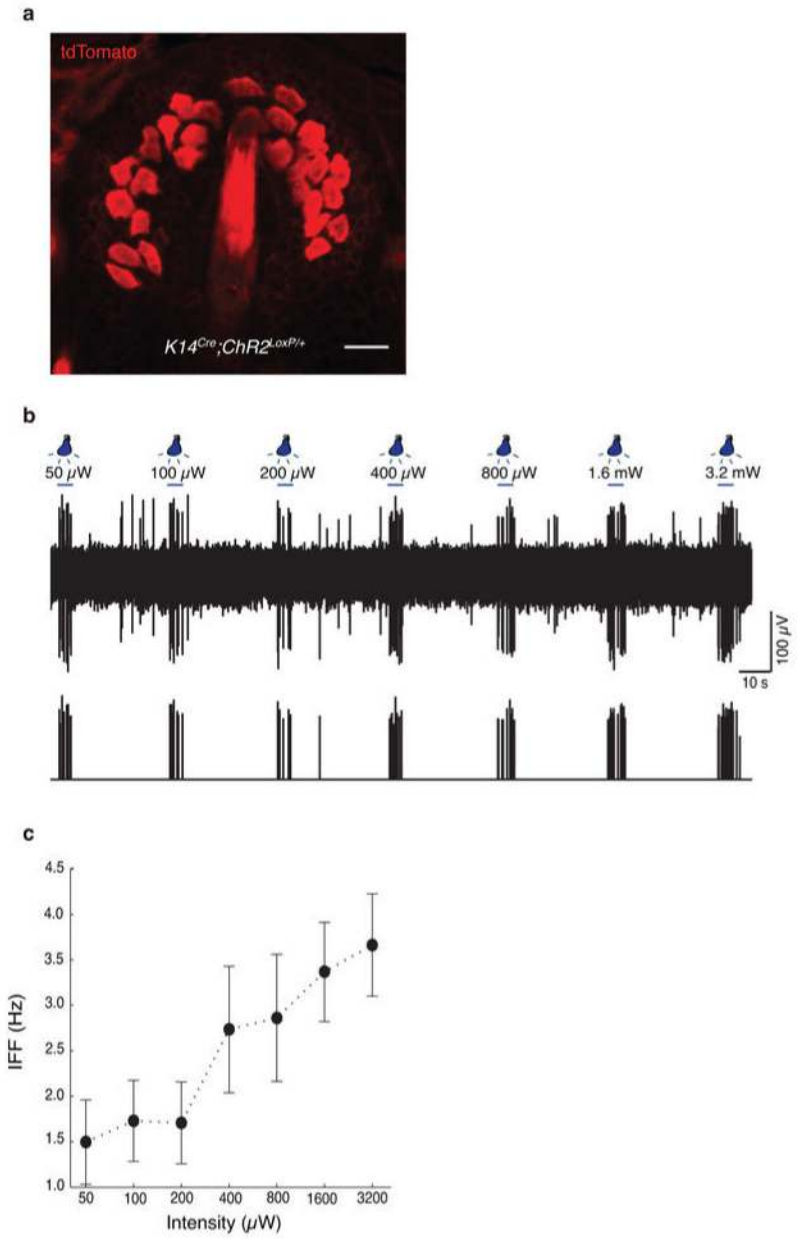

Extended Data Figure 5. *K14*^{Cre};*ChR2*$^{loxP/+}$ mice exhibit light-evoked SAI activity

a, Confocal image of a touch dome illustrating ChR2-tdTomato expression driven by *K14*^{Cre}. ChR2-tdTomato expressed much stronger in Merkel cells than in neighbouring keratinocytes. **b**, Light-evoked responses from the touch dome shown in **a** to seven light intensities as indicated. Spike sorting and clustering analysis were used to identify the unit that fired in phase with light (lower trace with spike positions and their amplitudes). **c**, Mean IFFs for light with varying illumination intensities on a log-intensity scale (*N*=3 recordings). Scale bar, 20 μm.

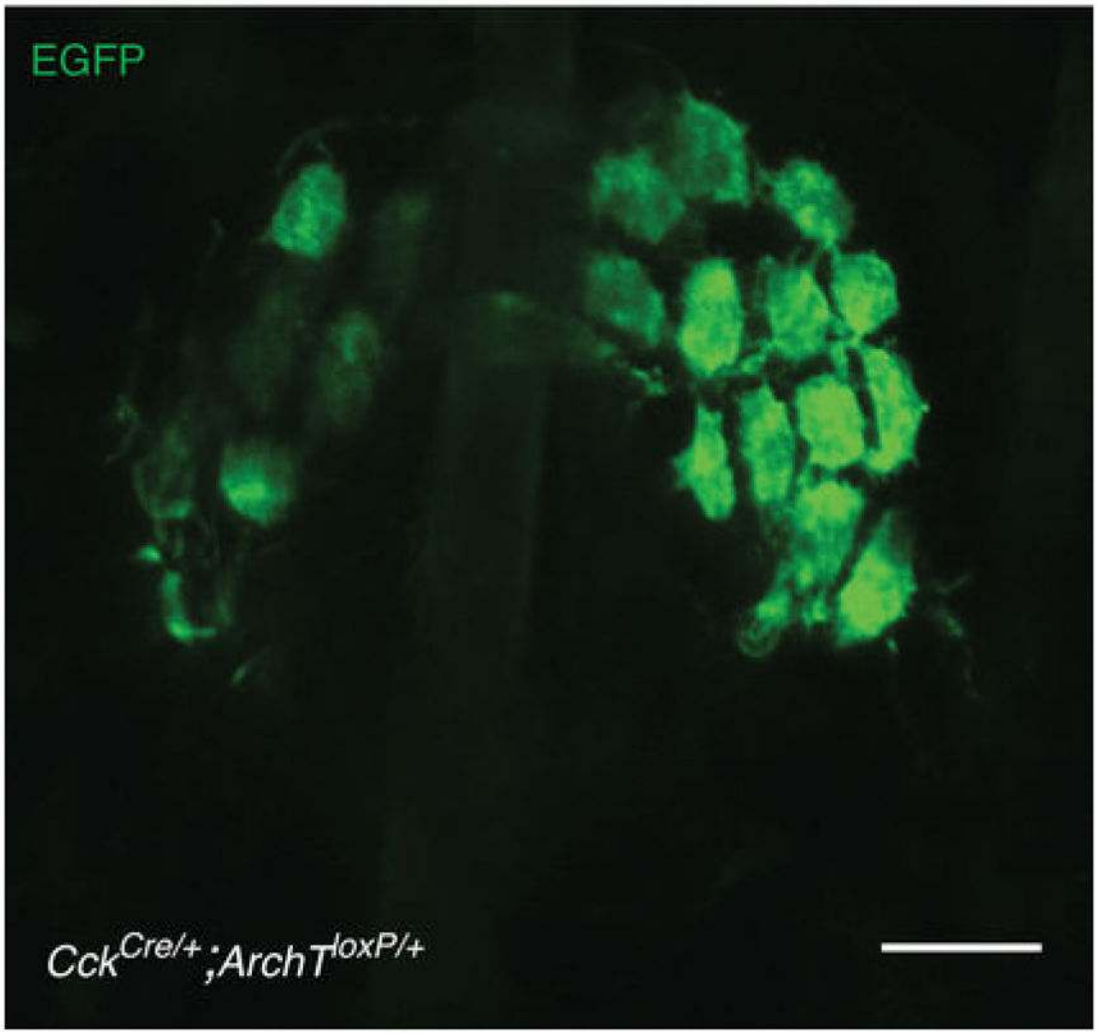

Extended Data Figure 6. Confocal axial projection of a touch dome shows selective ArchT-EGFP expression in Merkel cells driven by *Cck*^{Cre}

ArchT-EGFP expression was not observed in touch-dome afferents. Scale bar, 20 μm.

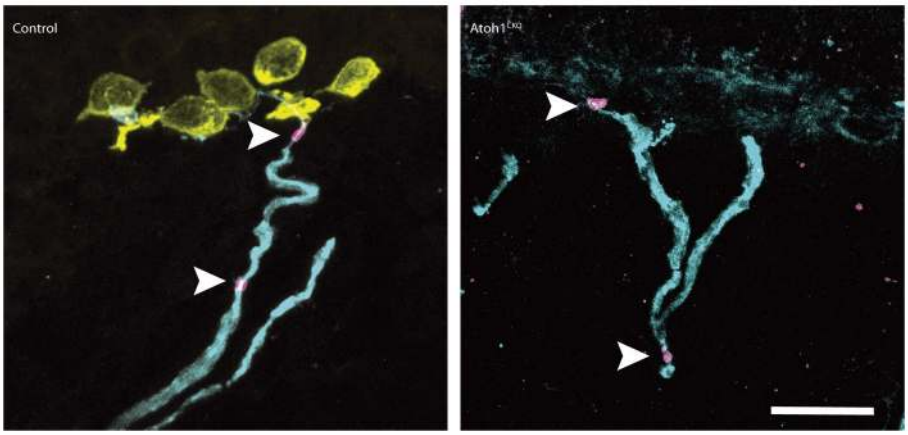

Extended Data Figure 7. Structure of touch-dome afferents in *Atoh1*^{CKO} mice

Immunostaining of skin cryosections from *Atoh1*^{CKO} and control genotypes are shown. Antibodies labelling myelinated afferents (NFH; cyan), Merkel cells (Keratin-8; yellow), nodes of Ranvier (βIV spectrin; magenta) show that the general structure of touch-dome afferents, including myelinated branches and Nodes of Ranvier (arrowheads), appears normal even in the absence of Merkel cells. Cell nuclei are labelled with DAPI (blue). Scale bar, 20 μm.

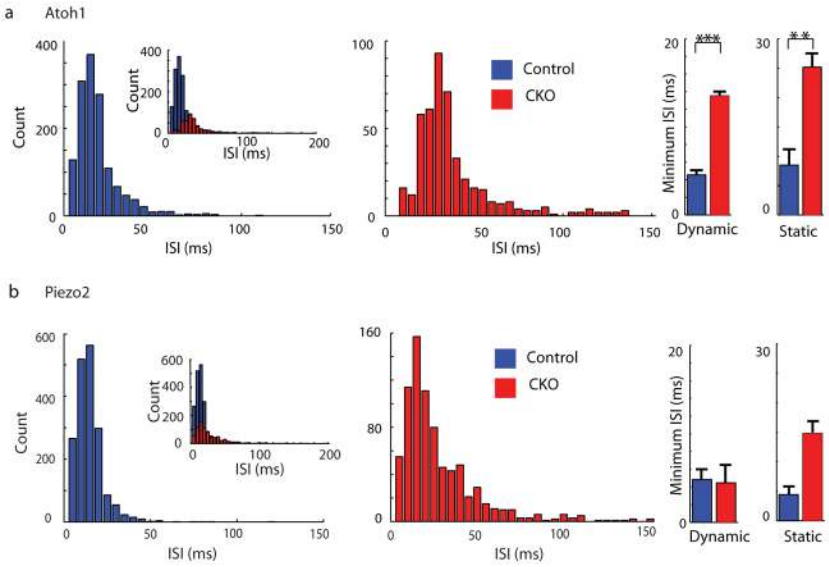

Extended Data Figure 8. Comparison of ISI distributions in *Atoh1*^{CKO}, *Piezo2*^{CKO}, and control genotypes

a, Histogram of ISI distribution during saturating responses in *Atoh1*^{CKO} (Mean±SD, 43.4±59.2 ms, Median: 29.8 ms; *n*=466 intervals from N=6 units) and control genotypes (Mean±SD, 16.5±12.9 ms, Median: 13.8 ms; *n*=1412 intervals from N=5 units). Inset on the left illustrates all ISIs, including those >150 ms, which were excluded from the main histograms [14/466 intervals in *Atoh1*^{CKO} and 1/1412 in control genotypes]. At right, bar graphs shows the minimum ISIs during dynamic and static phases. Minimum ISIs were longer in *Atoh1*^{CKO} than control mice for both phases, indicating a loss of high-frequency firing during dynamic stimuli and static displacement (**P<0.02, ***P<0.01; Student's *t* test). Mann-Whitney tests indicated that median values were also significantly different (P<0.001). **b,** Histogram of ISI distribution for *Piezo2*^{CKO} (Mean±SD, 41.9 ±32.3 ms, Median: 23.4 ms; *n*=792 intervals from *N*=6 units) and control genotypes (Mean±SD, 13.9±1.4 ms, Median: 11.8 ms; *n*=1845 intervals from *N*=5 units). Main histograms excluded long intervals (>150 ms; 4/792 intervals in *Piezo2*^{CKO} and 2/1845 in control mice.) Minimum ISIs were not significantly different in the dynamic phase (P ≥0.76; Student's *t* test and Mann-Whitney test); indicating that high-frequency firing is preserved in touch-dome afferents in these mice. For static phase firing, the means were not significantly different (P=0.095; Student's *t* test); however non-parametric analysis indicated that medians differed between genotypes (P=0.0043; Mann Whitney test).

Extended Data Table 1

Properties of mechanically and light-evoked currents in Merkel cells.
Activation kinetics (rise time, $t_{10–90\%}$) was estimated as the period from 10–90% of maximally evoked currents. Inactivation kinetics ($tau_{inactivation}$) were estimated by fitting single exponential functions 5 ms after I_{peak}. All values were estimated by linear interpolation at displacements nearest to the half-peak response. Measurements were conducted at V_h=−70mV.

		(mean ± SEM)
Mechanically activated	Mean peak current (pA)	370 ± 80
	Mean steady state current (pA)	20 ± 6
N = 6 6 trials	Rise time $t_{10–90\%}$ (ms)	1.0 ± 0.1
	$\tau_{inactivation}$ (ms)	8.1 ± 1.7
Light activated	Mean peak current (pA)	38 ± 2
	Mean steady state current (pA)	18 ± 1
N = 5 56 trials	Rise time $t_{10–90\%}$ (ms)	6.4 ± 0.4
	$\tau_{inactivation}$ (ms)	12 ± 1

Extended Data Table 2

Summary of touch-dome responses from ***Atoh1^{CKO}*** **and control mice.**
Maximum response among experimental set was chosen as representative data. Dynamic phase: period from stimulus onset (when the indenter began moving) to end of stimulation onset (indenter reaches the hold displacement depth). Static phase: initial 4s period after indenter reached commanded displacement. Unit of all values were milliseconds. Min: minimum, Max: maximum, Ave: averaged, SD: standard deviation, IA: Intermediately adapting response, CoV: coefficient of variation in static phase.

		Dynamic phase					Static phase						
	Data ID	# of spikes	Min (ms)	Max (ms)	Ave±SD (ms)	Median (ms)	# of spikes	Min (ms)	Max (ms)	Ave±SD (ms)	Median (ms)	Ratio of IA (%)	CoV
Atoh1 CKO	KO 1	41	15.4	24.5	19.3±2.3	19.5	132	20.9	53.3	30.1±5.0	29.8	33	0.16
	KO 2	37	15.4	61.8	27.3±10.6	25.1	56	27.1	300.1	69.2±51.9	49.0	50	0.75
	KO 3	49	6.2	594.3	35.2±88.9	13.6	39	10.6	667.3	101.0±137.1	50.9	100	1.36
	KO 4	31	15.0	42.8	22.9±5.9	22.6	26	28.4	71.4	42.6±9.7	41.8	100	0.23
	KO 5	18	15.5	33.6	22.4±5.2	23.6	24	26.1	233.8	58.0±46.6	41.5	100	0.80
	KO 6	35	19.3	26.4	23.2±3.5	23.5	12	32.1	286.8	98.6±74.9	61.7	100	0.76
Control	Wild 1	45	7.2	35.0	12.9±6.2	10.0	201	9.4	175.7	19.9±16.3	15.4	17	0.82
	Wild 2	77	4.2	81.7	18.7±11.4	16.4	95	22.0	95.4	42.0±13.2	39.1	0	0.32
	Wild 3	74	4.8	792.8	21.5±91.6	10.3	169	4.3	80.1	23.2±15.9	19.0	0	0.69
	Wild 4	89	3.3	11.5	4.9±1.8	4.0	274	3.9	48.2	14.5±7.2	13.1	0	0.51
	Wild 5	91	3.3	39.4	8.4±6.8	5.3	312	2.9	32.8	12.8±5.2	12.3	0	0.41

Acknowledgments

Thanks to Drs. Richard Axel, Amy MacDermott and the Lumpkin laboratory for helpful discussions, and to Danny Florez and Rebecca Piskorowski for advice on whole-cell recordings. Funding was provided by NIH/NIAMS grants R01AR051219 and R21AR062307 (to EAL), R01DE022358 (to AP) and fellowships to SM (5T32HL087745-05 and NIH/NINDS F32NS080544), MN (JSPS Research Fellowships for Young Scientists 24-7585), and AMN (McNair Foundation). Microscopy and flow cytometry was performed with Core support from Columbia SDRC (P30AR044535) and Cancer Center (P30CA013696). Initial studies were performed at Baylor College of Medicine with assistance from Flow Cytometry and Genetically Engineered Mouse Shared Resources (P30CA125123).

References

1. Johnson KO. The roles and functions of cutaneous mechanoreceptors. Curr Opin Neurobiol. 2001; 11:455–461. [PubMed: 11502392]
2. Lumpkin EA, Caterina MJ. Mechanisms of sensory transduction in the skin. Nature. 2007; 445:858–865. [PubMed: 17314972]
3. Kwan KY, Glazer JM, Corey DP, Rice FL, Stucky CL. TRPA1 modulates mechanotransduction in cutaneous sensory neurons. The Journal of neuroscience. 2009; 29:4808–4819. [PubMed: 19369549]
4. Haeberle H, et al. Molecular profiling reveals synaptic release machinery in Merkel cells. Proc Natl Acad Sci USA. 2004; 101:14503–14508. [PubMed: 15448211]
5. Maksimovic S, Baba Y, Lumpkin EA. Neurotransmitters and synaptic components in the Merkel cell-neurite complex, a gentle-touch receptor. Ann NY Acad Sci. 2013; 1279:13–21. [PubMed: 23530998]
6. Hartschuh W, Weihe E. Fine structural analysis of the synaptic junction of Merkel cell-axon-complexes. The Journal of investigative dermatology. 1980; 75:159–165. [PubMed: 6774030]
7. Iggo A, Muir AR. The structure and function of a slowly adapting touch corpuscle in hairy skin. J Physiol. 1969; 200:763–796. [PubMed: 4974746]
8. Woodbury CJ, Koerber HR. Central and peripheral anatomy of slowly adapting type I low-threshold mechanoreceptors innervating trunk skin of neonatal mice. J Comp Neurol. 2007; 505:547–561. [PubMed: 17924532]
9. Wellnitz SA, Lesniak DR, Gerling GJ, Lumpkin EA. The regularity of sustained firing reveals two populations of slowly adapting touch receptors in mouse hairy skin. J Neurophysiol. 2010; 103:3378–3388. [PubMed: 20393068]
10. Piskorowski R, Haeberle H, Panditrao MV, Lumpkin EA. Voltage-activated ion channels and Ca(2+)-induced Ca (2+) release shape Ca (2+) signaling in Merkel cells. Pflugers Arch. 2008; 457:197–209. [PubMed: 18415122]
11. Chalfie M. Neurosensory mechanotransduction. Nat Rev Mol Cell Biol. 2009; 10:44–52. [PubMed: 19197331]
12. Hu J, Lewin GR. Mechanosensitive currents in the neurites of cultured mouse sensory neurones. The Journal of physiology. 2006; 577:815–828. [PubMed: 17038434]
13. Coste B, et al. Piezo1 and Piezo2 are essential components of distinct mechanically activated cation channels. Science. 2010; 330:55–60. [PubMed: 20813920]
14. Walker RG, Willingham AT, Zuker CS. A Drosophila mechanosensory transduction channel. Science. 2000; 287:2229–2234. [PubMed: 10744543]
15. Woo SH, et al. Piezo2 is the Merkel cell mechanotransduction ion channel. Nature. 2014
16. Lesniak DR, et al. Computation identifies structural features that govern neuronal firing properties in slowly adapting touch receptors. Elife. 2014; 3:e01488.10.7554/eLife.01488 [PubMed: 24448409]
17. Boyden ES, Zhang F, Bamberg E, Nagel G, Deisseroth K. Millisecond-timescale, genetically targeted optical control of neural activity. Nat Neurosci. 2005; 8
18. Taniguchi H, et al. A resource of Cre driver lines for genetic targeting of GABAergic neurons in cerebral cortex. Neuron. 2011; 71:995–1013. [PubMed: 21943598]

19. Madisen L, et al. A toolbox of Cre-dependent optogenetic transgenic mice for light-induced activation and silencing. Nat Neurosci. 2012; 15:793–802. [PubMed: 22446880]
20. Quiroga RQ, Nadasdy Z, Ben-Shaul Y. Unsupervised spike detection and sorting with wavelets and superparamagnetic clustering. Neural Comput. 2004; 16:1661–1687. [PubMed: 15228749]
21. Dassule HR, Lewis P, Bei M, Maas R, McMahon AP. Sonic hedgehog regulates growth and morphogenesis of the tooth. Development. 2000; 127:4775–4785. [PubMed: 11044393]
22. Han X, et al. A high-light sensitivity optical neural silencer: development and application to optogenetic control of non-human primate cortex. Front Syst Neurosci. 2011; 5:18. [PubMed: 21811444]
23. Morrison KM, Miesegaes GR, Lumpkin EA, Maricich SM. Mammalian Merkel cells are descended from the epidermal lineage. Dev Biol. 2009; 336:76–83. [PubMed: 19782676]
24. Maricich SM, et al. Merkel cells are essential for light-touch responses. Science. 2009; 324:1580–1582. [PubMed: 19541997]
25. Meyers JR, et al. Lighting up the senses: FM1-43 loading of sensory cells through nonselective ion channels. The Journal of neuroscience. 2003; 23:4054–4065. [PubMed: 12764092]
26. Koltzenburg M, Stucky CL, Lewin GR. Receptive properties of mouse sensory neurons innervating hairy skin. Journal of neurophysiology. 1997; 78:1841–1850. [PubMed: 9325353]
27. Johnson KO, Lamb GD. Neural mechanisms of spatial tactile discrimination: neural patterns evoked by braille-like dot patterns in the monkey. The Journal of physiology. 1981; 310:117–144. [PubMed: 7230030]
28. Phillips JR, Johnson KO. Tactile spatial resolution. II. Neural representation of Bars, edges, and gratings in monkey primary afferents. Journal of neurophysiology. 1981; 46:1192–1203. [PubMed: 6275041]
29. Maricich SM, Morrison KM, Mathes EL, Brewer BM. Rodents rely on Merkel cells for texture discrimination tasks. J Neurosci. 2012; 32:3296–3300. [PubMed: 22399751]
30. Yamashita Y, Ogawa H. Slowly adapting cutaneous mechanoreceptor afferent units associated with Merkel cells in frogs and effects of direct currents. Somatosensory & motor research. 1991; 8:87–95. [PubMed: 1646558]
31. Lumpkin EA, et al. Math1-driven GFP expression in the developing nervous system of transgenic mice. Gene Expr Patterns. 2003; 3:389–395. [PubMed: 12915300]
32. Yang Y, Lacas-Gervais S, Morest DK, Solimena M, Rasband MN. BetaIV spectrins are essential for membrane stability and the molecular organization of nodes of Ranvier. The Journal of neuroscience. 2004; 24:7230–7240. [PubMed: 15317849]
33. Erturk A, et al. Three-dimensional imaging of solvent-cleared organs using 3DISCO. Nat Protoc. 2012; 7:1983–1995. [PubMed: 23060243]
34. Drew LJ, Wood JN, Cesare P. Distinct mechanosensitive properties of capsaicin-sensitive and -insensitive sensory neurons. The Journal of neuroscience. 2002; 22:RC228. [PubMed: 12045233]
35. Holt JR, Corey DP, Eatock RA. Mechanoelectrical transduction and adaptation in hair cells of the mouse utricle, a low-frequency vestibular organ. The Journal of neuroscience. 1997; 17:8739–8748. [PubMed: 9348343]
36. Lin JY. A user's guide to channelrhodopsin variants: features, limitations and future developments. Exp Physiol. 2011; 96:19–25. [PubMed: 20621963]
37. Haeberle H, Bryan LA, Vadakkan TJ, Dickinson ME, Lumpkin EA. Swelling-activated Ca2+ channels trigger Ca2+ signals in Merkel cells. PLoS One. 2008; 3:e1750.10.1371/journal.pone.0001750 [PubMed: 18454189]
38. Woo SH, Baba Y, Franco AM, Lumpkin EA, Owens DM. Excitatory glutamate is essential for development and maintenance of the piloneural mechanoreceptor. Development. 2012; 139:740–748. [PubMed: 22241839]

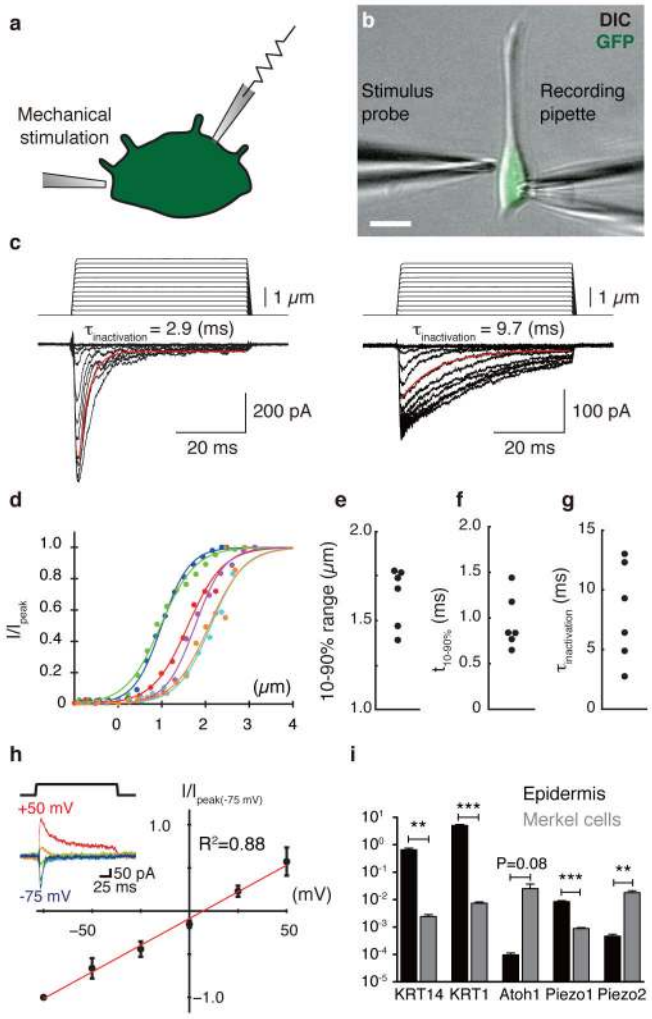

Figure 1. Merkel cells exhibit touch-evoked ionic currents and preferentially express Piezo2

a, Schematic of whole-cell recordings from dissociated Merkel cells[10]. **b,** Merkel cells were identified based on GFP fluorescence and were stimulated by a glass probe driven by piezoelectric actuator. Scale bar, 10 μm. **c,** Representative traces of mechanosensitive currents from two Merkel cells (V_{hold}=−70 mV). Inactivation kinetics were estimated from single-exponential fits (red lines). **d,** Current-displacement relationships from individual Merkel cells (*N*=6; indicated by distinct colors). Currents were normalized to peak and fitted with Boltzmann functions (R^2 > 0.97). **e–g,** Activation and inactivation kinetics and operating ranges for individual Merkel cells. **h**, Current-voltage relationship of mechanosensitive currents (*N*=5). Peak current at each holding potential was normalized to peak current at −75 mV. Reversal potential was estimated by linear regression (red line; R^2 = 0.88). Inset: representative traces at each holding potential (denoted by colors). **i,** qPCR analysis of Piezo1 and Piezo2 transcripts in purified Merkel cells and epidermis. Markers of keratinocytes (KRT14 and KRT1) and Merkel cells (Atoh1) verified selective enrichment of Merkel cells. **P<0.0001, ***P ≤0.001 (*N*=4).

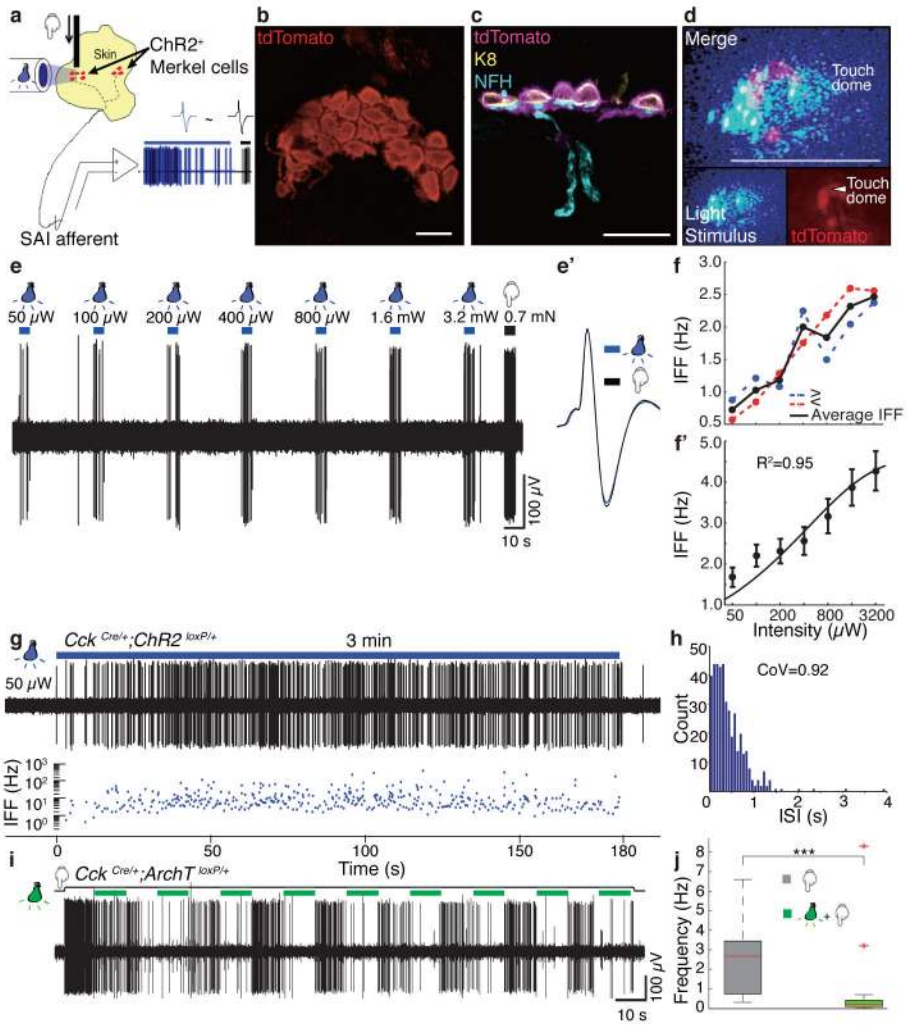

Figure 2. Merkel cells are necessary and sufficient to elicit sustained action-potential trains in touch-dome afferents

a, Schematic of mouse *ex vivo* skin-nerve recordings. **b,** Confocal image of a ChR2-expressing touch dome in a living skin-nerve preparation. Scale bar, 20 μm. **c,** Immunostaining of skin cryosections shows expression of ChR2-tdTomato in Merkel cells (Keratin-8, K8) but not in touch-dome afferents (Neurofilament heavy, NFH). Scale bar, 20 μm. **d,** During electrophysiological recording, ChR2-expressing Merkel cells and blue-light stimuli were imaged separately using different filter sets (bottom insets). Merged image illustrate**s** the illuminated area (top panel). Confocal reconstruction of this touch dome is in Extended Data Fig. 2a–e. Scale bar, 200 μm. **e,** Light pulses of increasing intensities elicited phase-locked action potentials from the touch dome in **d. e′,** Comparison of spike shapes evoked by light (blue) and touch (black) confirmed single-unit recording. **f,** Mean instantaneous firing frequency (IFF) versus light intensity for a single touch-dome afferent. Blue trace shows mean IFFs from **e**. Red trace shows mean IFFs evoked by light intensities presented in decreasing order. The averages of these stim**uli (black) were** analysed further. **f′,** Mean IFFs on a log-intensity scale (*N*=12 single units). Data were fit with a four-parameter Weibull sigmoidal function (R^2=0.95). **g–h,** A sustained light-evoked response

from the touch-dome afferent **in d–e** with corresponding ISI histogram. **i–j,** Optogenetic silencing of ArchT-expressing Merkel cells. **i,** Representative 3-min recording. **j,** Box-plot of firing rates during light-off (*N*=3 units, *n*=20 10-s periods) and light-on (same units, *n*=23 10-s periods). Two outliers are firing rates from initial light-on periods. P=0.001.

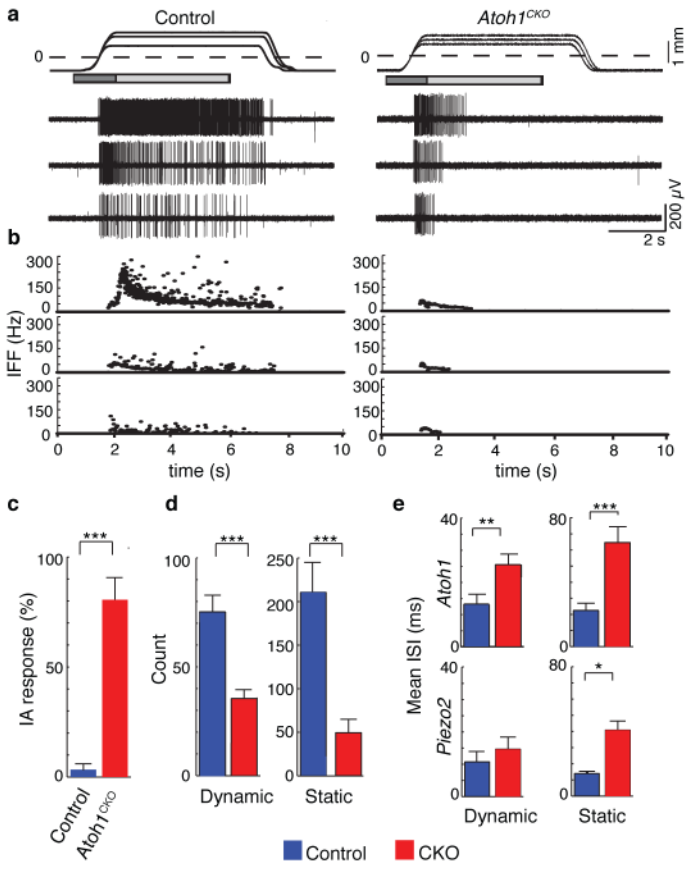

Figure 3. *Atoh1*^{CKO} and *Piezo2*^{CKO} mice show intermediately adapting (IA) responses

a, Mechanically evoked responses from touch-dome afferents in control and *Atoh1*^{CKO} (*K14*^{Cre};*Atoh1*$^{LacZ/flox}$) mice. Top trace shows ramp-and-hold displacements at three magnitudes with corresponding action potential trains below. Dashed line marks the point of skin contact (0 mm). Boxes indicate dynamic (dark gray: 1.5 s after displacement command onset) and static phases for analysis (light gray: 4 s after the beginning of hold command). **b,** IFFs of the responses in **a. c,** Proportion of IA responses to supra-threshold displacements in touch-dome afferents (*N*=5 control and *N*=6 *Atoh1*^{CKO} units). **d,** Mean number of spikes in dynamic and static phases of saturating responses. **e,** Mean interspike intervals (ISIs) of *Atoh1*^{CKO} (*N*=6 units), *Piezo2*^{CKO} (*N*=6 units) and their respective control genotypes (*N*=5 units per genotype). Asterisks indicate statistically significant differences between mutant and control genotypes in Fisher's exact test (**c**) and Student's *t* test (**d–e**). *P<0.05; **P<0.02; ***P<0.01.

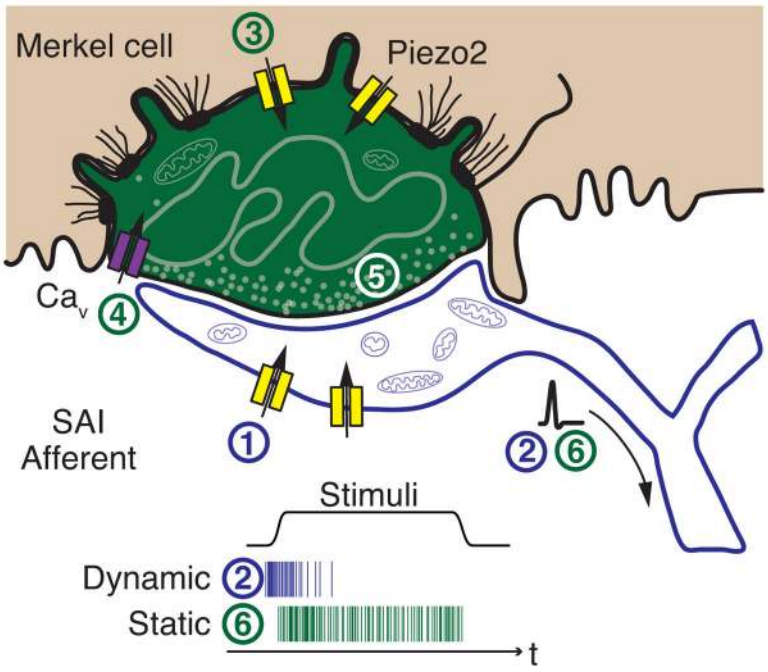

Figure 4. Model of active Merkel-cell inputs in touch reception

Deformation of the skin opens mechanotransduction channels in SAI afferents (1) to initiate action potential firing at the onset of dynamic stimuli (2). The presence of Merkel cells boosts dynamic firing through Piezo2-independent mechanisms. Skin deformation simultaneously activates Piezo2-dependent[15] mechanotransduction channels in Merkel cells (3) to depolarize these cells, which produces calcium entry (4) and release of unidentified neurotransmitters (5) that trigger sustained firing (6). Schematic after Iggo and Muir[7].